J Mater Sci: Mater Med (2011) 22:2513–2523
DOI 10.1007/s10856-011-4425-1

Crystallinity assessment and in vitro cytotoxicity of polylactide scaffolds for biomedical applications

J. R. Sarasua · N. López-Rodríguez · E. Zuza · S. Petisco · B. Castro · M. del Olmo · T. Palomares · A. Alonso-Varona

Received: 24 May 2010 / Accepted: 11 August 2011 / Published online: 21 August 2011

Abstract Bioresorbable polylactides are one of the most important materials for tissue engineering applications. In this work we have prepared scaffolds based on the two optically pure stereoisomers: poly(L-lactide) (PLLA) and poly(D-lactide) (PDLA). The crystalline structure and morphology were evaluated by DSC, AFM and X-ray diffraction. PLLA and PDLA crystallized in the α form and the equimolar PLLA/PDLA blend, crystallized in the stereocomplex form, were analyzed by a proliferation assay in contact with mouse L-929 and human fibroblasts and neonatal keratinocytes for in vitro cytotoxicity evaluation. SEM analysis was conducted to determine the cell morphology, spreading and adhesion when in contact with the different polymer surfaces. The preserved proliferation rate showed in MTT tests and the high colonization on the surface of polylactides observed by SEM denote that PLLA, PDLA and the equimolar PLLA/PDLA are useful biodegradable materials in which the crystalline characteristics can be tuned for specific biomedical applications.

J. R. Sarasua (✉) · N. López-Rodríguez · E. Zuza · S. Petisco
Department of Mining-Metallurgy and Materials Science, School of Engineering, University of the Basque Country (UPV/EHU), 48013 Bilbao, Spain
e-mail: jr.sarasua@ehu.es; ana.alonsovarona@ehu.es

B. Castro · M. del Olmo
Histocell S. L., Derio, Spain

T. Palomares · A. Alonso-Varona
Faculty of Medicine and Odontology, University of the Basque Country (EHU-UPV), Bilbao, Spain

1 Introduction

One approach for tissue engineering [1, 2] involves harvesting of autologous cells from the patient. Cells are at first cultured on a scaffold in vitro and then implanted with the scaffold in the defect of the patient where the tissue should regenerate at the rate at which the scaffold reabsorbs [3]. In this field, due to anchorage dependence of most cells in tissues and organs in vivo, it is essential to combine adequate scaffolds and proliferating cells. These scaffolds should primarily possess an adequate surface chemistry and allow cell attachment, proliferation and growth.

Up to now different polymers as well as processing techniques have been used to develop scaffolds for tissue engineering [4]. Aliphatic polyesters, such as polyglycolic acid (PGA), polylactic acid (PLA) and poly(ε-caprolactone) (PCL) or their copolymers have been used for in vitro cytotoxicity studies [5–9] covering a range of mechanical properties and degradation profiles. In spite of the fact that good results were obtained, the lack of mechanical stability or the release of acid degradation products could adversely affect cell viability [9].

Thermoplastic aliphatic biodegradable polyesters based on lactic acid, known as poly(lactic acid)s or polylactides or simply PLAs, are receiving attention by the biomedical field in applications areas such as sutures, antibiotic release systems, macroscopic temporary implants and scaffolds for tissue engineering [10, 11]. Polylactides are usually obtained by ring opening polymerization of lactide, a molecule containing two chiral carbon atoms that provide the possibility of having different type optical activity and crystalline development. The presence of asymmetrical carbon atoms [12] in polylactide chain structure leads to the existence of different stereoisomers. Optically pure

polylactides, poly(L-lactide), hereafter called PLLA, and poly(D-lactide), PDLA, show stereoregular moiety distribution all over their chain and therefore are semicrystalline polymers. If however there is only some degree of regularity in the LL/DD moiety distribution then polylactides can be regarded as copolymers whose crystallization ability decreases with optical purity [13]. Finally, optically non-active polylactides result from racemic or meso monomers so they can be regarded as *atactic* copolymers with random moiety distribution in the chains and because of this structural irregularity are amorphous polymers (PDLLAs).

A remarkable feature of polylactides is also their crystal polymorphism [14–21]. Optically pure polylactides are reported to crystallize in a pseudo-orthorhombic crystal form (the so called α allotrope). The α crystal lattice contains segments of two identical 10_3 helical chains with ten monomer units intervening per three turns [15, 16]. However, optically non-pure polylactides (for instance the enantiomeric blends or the stereocopolymers) can also crystallize as stereocomplex (η polymorph); in this case the crystal lattice is triclinic and contains L-lactide and D-lactide segments of chains in 3_1 helical conformation [17, 18]. The stereocomplexation observed in polylactide enantiomeric blends can be explained by the higher compaction induced by intermolecular interactions between units of opposite configuration. In a recent work we demonstrated that H-bonding forces causing specific $CH_3\cdots O{=}C$ and $C_\alpha H\cdots O{=}C$ interactions between both stereoisomers of polylactide are the driving force for stereocomplexation of enantiomeric polylactide chains [19].

Crystallinity is a well known material variable that affects not only the physical–mechanical properties but also biodegradability. In the case of polylactides crystalline stereocomplexation has been reported to provide higher thermal stability, which can be useful for thermal sterilization processes but also brings with it mechanical brittleness [20, 21]. It is also well known that biodegradation rate is slower in semicrystalline than in amorphous samples [22, 23], hence, biodegradation rate decreases with higher crystallinity index. In addition, biodegradation has been reported to be reduced in polylactide stereocomplex crystals compared to homocrystals [24, 25].

Crystal morphology of polylactides is also the result of the manufacturing method used and the thermal treatment applied during conformation. Polylactides crystallized from the melt show spherulitic morphology. Higher spherulite sizes and lamellar thickness result from crystallizations conducted at low undercoolings from the melt [13]. However, when recrystallized by annealing after a solvent casting preparation, the polylactide films show different micro- and nano-structural characteristics [26]. Crystalline morphologies of thin films of PLLA crystallized from the melt can be provided by atomic force microscopy (AFM) showing the formation of S-shaped edge-on lamellae during the initial stages of crystallization [27, 28]. As the crystals grow, a transition from edge-on to flat-on crystals was observed; afterwards, crystallization proceeded only through flat-on crystals. The curved morphology of less perfect crystals in the core region of spherulites is responsible for the lower thermal stability and the lower hydrolytic resistance relative to the flat on crystals located in the outer regions, as evidenced by the micrographs taken by Fischer et al. showing degradation of the centre of the spherulites in significant extent compared to the outer regions [29].

Some studies on cell response to roughness and surface morphology [30, 31] and crystallinity [32, 33] have already been conducted on PLLA. For instance, processing techniques that leaded to seemingly inconsequential changes in bulk and surface properties were found to influence biological response [32], and different cellular response was found in vitro and in vivo for PLLAs of seemingly same crystallinity [33]. Nevertheless, how the complex nanoscale structural features of semicrystalline polymers affect cell functions as a part of topography is not understood yet. It is reported that individual cells recognize structures which have comparable dimensions to cellular size (10–100 μm) [34]. Hence microscale surface morphological textures associated to crystallinity need also to be considered among the design criteria of scaffolds for tissue engineering.

The crystalline characteristics of polylactides can be modelled by selecting different stereoisomers and hybridization procedures such as copolymerization and blending, however how the resulting micro- and nano-structures can condition biocompatibility is not understood yet [34]. The aim of the present study is to determine the effects on cell response to surface chemistry derived from the different chirality and crystalline structure and morphology of polylactides. A recent study on the responses of osteoblastic cells to polylactide substrates of different chirality probed that racemic stereocomplex crystals formed with PLLA and PDLA showed relatively higher positive effects on both cell growth and proliferation, whereas the effect of PDLA was negative [35].

In this work scaffolds of PLLA, PDLA and the stereocomplexed equimolar enantiomeric PLLA/PDLA blend are analysed by putting them into contact with L929 murine fibroblasts, human neonatal fibroblasts and keratinocytes. Cell culture matrices improve the understanding of basic cell biology, however the surface chemistry and crystalline characteristics of the scaffolds still need to be evaluated. Hence in this work the effects of chirality and resulting crystalline characteristics of polylactides have been determined in terms of cell attachment, proliferation and growth in vitro.

2 Experimental part and methods

2.1 Starting materials

Poly(L-lactide) *BiomerL9000*® having molecular weight $M_w = 205.000$ g/mol and polydispersity index (PI) 1.58 was supplied by *Boehringer Ingelheim* (Germany). PDLA *Purasorb PD 57*® having molecular weight $M_w = 349.000$ g/mol and polydispersity index (PI) 1.92 was supplied by *Purac Biochem* (The Netherlands).

2.2 Preparation of films

PLLA and PDLA pellets were dried in a vacuum oven at 60°C overnight. Both PLLA and PDLA dissolve in chloroform and remain stable at room temperature. All films used to assess in vitro cytotoxicity and for SEM were prepared in same way. Polylactide films of ~80 μm thickness were obtained from same volumes of 2 wt% solutions in chloroform. PLLA, PDLA and the equimolar mixture of PLLA and PDLA (hereafter named B-5050) films were prepared by casting the polylactide solutions into petri dishes. The films were dried for 24 h in air at room conditions and then placed into a vacuum at 30°C to assure the complete evaporation of the solvent.

2.3 Thermal treatment and sterilization of samples

Both PLLA and PDLA films were annealed at 120°C for 1 h. This is because PLLA and PDLA crystallize as α homocrystals and 1 h of annealing at 120°C was found enough to develop their crystallinity. However, the equimolar B-5050 blends were submitted to annealing at 190°C for 4 and 8 h in order to develop selectively the stereocomplex crystallinity under favourable conditions [20]. The heat treatment strategy is aimed at evaluating the effect of polymorphism on cytotoxicity. Hence, PLLA (or PDLA) and B-5050 scaffolds have been specifically crystallized to have different polylactide crystal polymorphs. Thermal sterilization of films was finally conducted in an autoclave at 120°C for 20 min before using these polylactide films of defined crystallinity in cytotoxicity assays and SEM.

2.4 Differential scanning calorimetry

Thermal analysis was carried out on a DSC from TA Instruments, model DSC 2920. Approximately 5 mg of each material was weighed and sealed in an aluminium pan. A 0–250°C temperature range was used. Melting temperature (T_m), glass transition temperature (T_g) and enthalpy of crystal fusion (AH_f) were determined at 10°C/min. The thermal characterization by DSC was carried out before and after sterilization of the films. In the as cast films, a cold crystallization exotherm was observed (T_c), hence a cold crystallization enthalpy (AH_c) was also determined. The crystallinity index was calculated from the net enthalpy using 106 and 142 J/g as standard enthalpy values for fully crystalline homo- and stereo-complex crystals [19].

2.5 Atomic force microscopy

Atomic force microscopy images were recorded at room temperature using a Nanoscope IIIa Multimode Scanning Probe Microscope (Veeco Instruments, Santa Barbara, CA). AFM was operated in tapping mode. Samples were obtained by casting a polylactide solution onto a sample mounting disk, in some cases annealed in an oven according to a recrystallization strategy, and tested using a phosphor doped silicon cantilever (*Rtespa* model, Veeco) with nominal spring constant of 40 N/m and operating frequency of 300 kHz. The obtained films were approximately 8 μm thick. The small radius of the probes ($R < 10$ nm) allowed the acquisition of high resolution images. The scanning rate used was 0.5 Hz.

2.6 Wide angle X-ray diffraction

The X-ray powder diffraction patterns were collected by using a PHILIPS X'PERT PRO automatic diffractometer in theta-theta configuration, secondary monochromator with Cu-K_α radiation ($\lambda = 1.5418$ Å) and a PIXcel solid state detector. The sample was mounted on a zero background silicon wafer fixed in a generic sample holder. Data were collected from 10 to 25° 2θ (step size = 0.026 and exposure time = 0.8 s) at room temperature.

2.7 Cells

Three types of cells were used: Fibroblasts L929 and human neonatal fibroblasts and keratinocytes. Cells were cultured in a humidified atmosphere (5% CO_2, 95% air) at 37°C. Exponentially growing cell cultures were used in all experiments. After a brief exposure to phosphate-buffered saline (PBS)–ethylenediaminetetraacetic acid (EDTA) (2 mmol/l) and centrifuging, the pellet was resuspended in Hank's solution and cells were enumerated with a Coulter counter. Viability, as determined by Trypan blue exclusion, ranged from 95 to 98%.

L929 cells used as control were purchased from American Type Culture Collection (ATCC) and maintained in Dulbecco's minimum essential medium (DMEM) supplemented with 10% Fetal Calf Serum (Biochrom), 2 mM glutamine and 1% antibiotic–antimycotic (Bio Whittaker, Cambrex).

Human neonatal fibroblasts and keratinocytes were obtained from clinical biopsy. Tissue fragments were excised aseptically and transferred into antibiotic-fungizone solution. After transport, the fragments were transferred into fresh solution. This washing procedure was repeated three times. Skin fragments of 2 × 2 cm were incubated overnight at 4°C in Splitting solution (dispase 25 U/ml) (Cascade Biologics). Epidermis was treated with trypsin–EDTA (0.025–0.01%) at 37° for 30 min. Keratinocytes obtained were washed, counted and maintained in defined Keratinocyte-SFM Growth Supplement (Gibco BRL Co.). Dermis was incubated in Collagenase I (2 mg/ml) at 37°C for 2 h. Dermal fibroblasts obtained were cultured in 106 Medium supplemented with Low Serum Growth Supplement kit (Cascade Biologics).

2.8 Preparation of extracts of test materials

In all tests, we used polymer films sterilized by ethylene oxide of thickness ≤100 μm. The ratio of material surface to extract fluid was constant and equal to 6 cm^2/ml, according to ISO 10993-12 [36], and the time of extraction was 24 h at 37°C in a humidified atmosphere containing 5% CO_2. To provide the basis for a comparison of the effects of the test material, we used also a negative control (High-Density PolyEthylene, USP Rockville, USA) and a positive control (Polyvinyl chloride, Portex Ltd, UK).

2.9 Cytotoxicity assays

To assess the short-term cytotoxicity of the developed polylactides, ISO/EN 10993 part 5 guidelines were used: Medium extraction with a 24 h extraction period and MTT assay to establish the possible toxic effects of leachables released from polymers during extraction [37]. L929 cells, keratinocytes and fibroblasts (4000 cells/well) were plated in 96-well clusters which were used for cytotoxicity assays. All cultures were incubated in corresponding medium for 24, 48, and 72 h. Toxicity was determined by a colorimetric assay (Cell Proliferation Kit I MTT, Roche). Briefly, viable cells could reduce the MTT to formazan pigment, which was dissolved by 1 ml dimethyl sulphoxide (DMSO) after removal of the culture medium. The cell number per well was proportional to the absorbance recorded at 570 nm using an ELISA plate reader. Experiments were performed by triplicate and each assay was repeated three times.

2.10 Direct contact assays by SEM

The adhesion and morphology of L929 cells, human neonatal keratinocytes and fibroblasts was assessed by SEM. Cells were grown as monolayer cultures as described previously until they reached P5 (passage 5). At that time, cells were detached, centrifuged and resuspended in cell culture medium. Aliquots containing 5 × 10^4 cells were seeded on top of the polymers, placed previously in 24 well ultra low cluster flat bottom culture plates (Costar). After 24 h, samples were fixed with 2% glutaraldehyde in cacodylate buffer (0.1 M pH = 7.4) for 2 h at room temperature and post-fixed in 1% OsO_4 for 1 h, washed in PBS and subjected to a graded ethanol series and dried through the CO_2 critical point. Finally, samples were sputter-coated with a thin layer of gold and observed in a Hitachi SEM (Hitachi S-3400 N). The voltage used was 15.0 kV. The working distance was ranging from 16.0 to 16.7 mm, depending on the sample. Relating to magnification used for SEM images, we used 1500× in the case of murine L-929 fibroblasts, in neonatal fibroblasts we used 400× due to the bigger size of the cells and, finally, for neonatal keratinocytes, the magnification was 1500×.

2.11 Statistics

Student's *t*-tests were used to assess the statistical differences between groups at different time points. Values were considered to be statistically different from controls when $P < 0.05$ for a 95% confidence interval.

3 Results

3.1 Crystallinity of polylactides as determined by DSC, X-ray diffraction and AFM

Figure 1 shows the DSC traces of optically pure polylactides as cast, referred as PLLA1 and PDLA1, and after the sterilization in autoclave at 120°C for 20 min (PLLA2 and PDLA2). PLLA1 and PDLA1 show the heat jump corresponding to the T_g at 26.4 and 30.6°C, respectively followed by a typical cold crystallization peak located at 75.2 and 77.4°C. The low T_g observed is a result of the casting-evaporation method used for processing the scaffolds and indicates that the evaporation of chloroform during drying leaves higher free volume in polylactide. The melting peak is also observed, centred at 157.2°C in PLLA1 and centred at 174.4°C in PDLA1. The lower value of melting temperature of PLLA is due to the lower molecular weight and the existence of a 0.2 wt% enantiomer residue leading to chain stereoirregularity that depresses the melting point in regard to optically pure polylactides [13].

The DSC traces of sterilized samples are quite different. As a result of the crystallinity developed during the thermal sterilization process in the autoclave the glass transitions of PLLA and PDLA appear at considerably higher

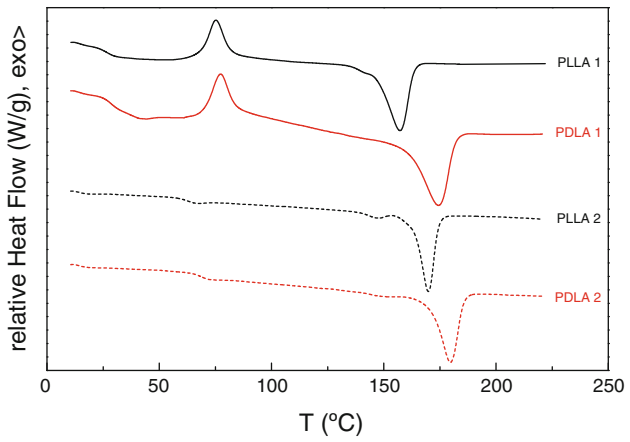

Fig. 1 DSC traces of optically pure PLLA and PDLA before and after thermal sterilization in an autoclave at 120°C for 20 min

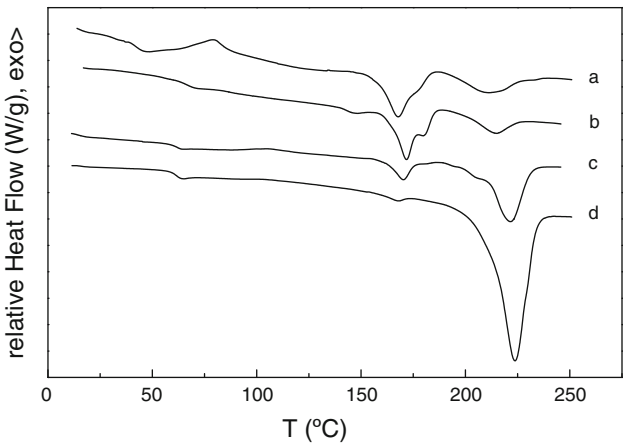

Fig. 2 DSC traces of the equimolar PLLA/PDLA blend: (*a*) as cast, (*b*) sterilized, (*c*) recrystallized at 190°C for 4 h, (*d*) recrystallized at 190°C for 8 h

temperature than in the previous case, respectively at 62.4 and 68.7°C. Sterilized samples did not show cold crystallization during DSC indicating that the crystallization process was completed in the autoclave. The melting temperatures of sterilized PLLA and PDLA appear at 169.8 and 179.7°C respectively, several degrees above those above mentioned, as expected from the completed crystallization in the autoclave. In addition a remarkable feature is also detected in both sterilized samples since just before the melting a small T_g *like* transition (located at 146.9°C in PLLA and at 150.0°C in PDLA) is observed, subsequently followed by a small exothermic event. The former is an endothermic transition that some authors have named *annealing peak* [38] and can be observed in semicrystalline polymers after isothermal crystallization or annealing at a temperature between T_g and the melting temperature. This transition can be associated to a low temperature melting of imperfect crystals or to a relaxation corresponding to a rigid amorphous phase. The latter is occurring just before the melting and has been attributed to a perfectionment process of a more imperfect crystalline form of polylactide that recrystallizes in a more perfect crystal polymorph [39].

Table 1 summarizes the thermal properties of optically polylactides before and after sterilization determined by DSC. The crystallinity index (X_c) of the above described samples was calculated with the following equation:

$$X_c\,(\%) = \frac{\Delta H_m - \Delta H_{c1} - \Delta H_{c2}}{\Delta H_m^0} \cdot 100 \qquad (1)$$

ΔH_m is the measured melting enthalpy and ΔH_{c1} and ΔH_{c2} are the exothermal enthalpy values corresponding to the cold crystallization and recrystallization occurring just before the melting. $\Delta H_m^0 = 106$ J/g was taken according to bibliography [13]. As can be observed both as cast polylactides (PLLA1 and PDLA1) are nearly amorphous showing low crystalline fraction, however the crystallinity increases up to 27.9 and 32.6% respectively for PLLA2 and PDLA2 sterilized in the autoclave at 120°C for 20 min.

Figure 2 shows the DSC traces of equimolar PLLA/PDLA (B-5050) blends (a) as cast (b) recrystallised at 120°C for 20 min, (c) recrystallised with annealing at 190°C for 4 h, and (d) recrystallised with annealing at 190°C for 8 h. As can be observed a T_g at 32.5°C followed by cold crystallization is observed in the as cast sample. The sterilised and annealed samples show typical T_g value at 67.3°C with no subsequent cold crystallization and a second T_g *like* transition at 143.1°C, attributed to a relaxation of a rigid amorphous phase. Finally double melting

Table 1 Thermal properties including the crystallinity index (X_c) of PLLA and PDLA before and after sterilization in an autoclave at 120°C for 20 min

Sample	T_{g1} (°C)	T_{g2} (°C)	T_c (°C)	ΔH_{c1} (J/g)	ΔH_{c2} (J/g)	T_m (°C)	ΔH_m (J/g)	X_c (%)
PLLA 1	26.4	–	75.2	14.6	–	157.2	27.8	12.4
PLLA 2	62.4	146.9	–	–	1.1	169.8	30.7	27.9
PDLA 1	30.6	–	77.4	16.4	–	174.4	27.3	10.3
PDLA 2	68.7	150.0	–	–	0.6	179.7	35.3	32.7

Table 2 DSC thermal properties including the stereocomplex crystalline fraction (X_S) and overall crystallinity index (X_c) for the equimolar PLLA/PDLA blend

Sample	T_{g1} (°C)	T_{g2} (°C)	T_c (°C)	ΔH_c (J/g)	T_m(H) (°C)	ΔH_m(H) (J/g)	T_m(S) (°C)	ΔH_m(S) (J/g)	X_S (%)	X_c (%)
"Casting"	32.5	–	77.7	7.9	167.8	20.6	209.4	4.6	18.3	15.3
Sterilised	67.3	143.1	–	–	171.8	23.0	214.3	9.9	30.1	28.2
(4 h—190°C)	62.4	–	–	–	167.6	2.0	222.3	63.1	96.9	46.2
(8 h—190°C)	62.0	–	–	–	167.5	0.9	222.9	73.9	98.8	52.8

was observed in PLLA/PDLA blends with a low melting peak ranging 167.5–167.8°C, and a high melting peak ranging 209.4–222.9°C depending on thermal treatment. Table 2 summarizes the thermal properties of these B-5050 blends including the homocrystal/sterocomplex crystalline fraction that was calculated according to bibliography [20]. It is noted that as cast and sterilised samples contain a higher fraction of α homocrystals; however, the stereocomplex crystal fraction increases with annealing time at 190°C attaining approximately 100% in 8 h.

Figure 3 shows the X-ray diffraction patterns of optically pure PLLA as cast and recrystallized during sterilization at 120°C (bottom curves) and those of the equimolar mixture of optically pure poly(L-lactide) and poly(D-lactide) (PLLA/PDLA) as cast and after stereocomplexation by annealing at 190°C for 1 and 24 h (top curves). PDLA patterns are not shown because they are equivalent to those introduced for PLLA. It can be noted that as cast PLLA is practically amorphous whereas the sterilized optically pure non-blended PLLA is semicrystalline showing its most intense peak at a $2\theta = 16.6°$ due to reflections from (200) and/or (110) planes. Less intense peaks were also observed at $2\theta = 14.7°$, 18.9° and 22.1° corresponding respectively to reflections of (010), (203) and (015) planes. These results are in close agreement with the peaks reported in the literature for the α polymorph. The as cast equimolar blend of optically pure PLLA and PDLA revealed a hybrid crystalline development with the most intense peak at $2\theta = 16.6°$ due to reflections of (200) and/or (110) of the α crystal polymorph, yet a small diffraction peak at 12° indicates the presence of a small amount of stereocomplex. The equimolar blend annealed at 190°C showed a very different X-ray pattern. In the case of the 1 h annealed sample the most intense diffraction peaks reveal that both α (peak at 16.6°) and η polymorphs (peaks at 12°, 21° and 24° due to reflections of (101), (204) and (211) planes) are present. It is also to be noted that very close to the 16.6° peak attributed to reflections of the α crystal appeared a peak at 16.4° that is attributed to (110) reflections of the stereocomplex crystal [20]. For the 8 h annealed equimolar blend, the peak at 16.6° nearly vanishes and the most intense peaks appear at 12°, 16.4°, 21° and 24°, indicating that the stereoselective crystallization in the form of stereocomplex has been achieved.

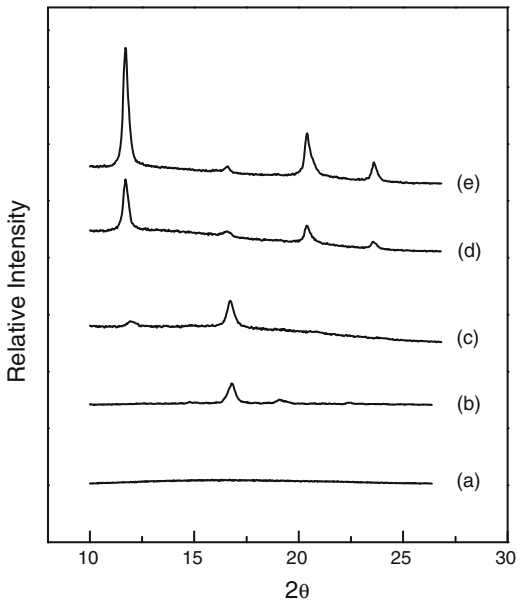

Fig. 3 X-ray diffraction patterns of PLLA and B5050: (*a*) PLLA as cast, (*b*) PLLA sterilized, (*c*) B5050 as cast, (*d*) B5050 recrystallized at 190°C for 1 h, (*e*) B5050 recrystallized at 190°C for 8 h

The crystalline morphology of polylactides was determined by AFM. Figure 4 shows height image (left side) and phase image (right side) of PLLA as cast (a, b) and recrystallized under thermal conditions of autoclave sterilization at 120°C for 20 min in a vacuum oven (c, d). Spherulites of 5–6 μm diameter with radial growth of edge-on lamellae are observed in the as-cast film. The average thickness of lamellae was estimated being approximately 100–150 nm. In addition a significant amount of non-crystallised amorphous inter-lamellar and inter-spherulitic dark regions are relevant, in agreement with the low crystallinity corresponding to the as cast samples. However, the PLLA films crystallized under sterilization conditions revealed a sheaflike morphology constituted of axiallites (also called hedrites) [40] that represent an intermediate stage in the formation of spherulites. The average thickness of lamellae in this case was estimated being approximately 70–100 nm.

In order to assess a 3D representation of the crystalline morphologies a section analysis was conducted on both as cast and sterilized samples. Figure 5a, b shows respectively

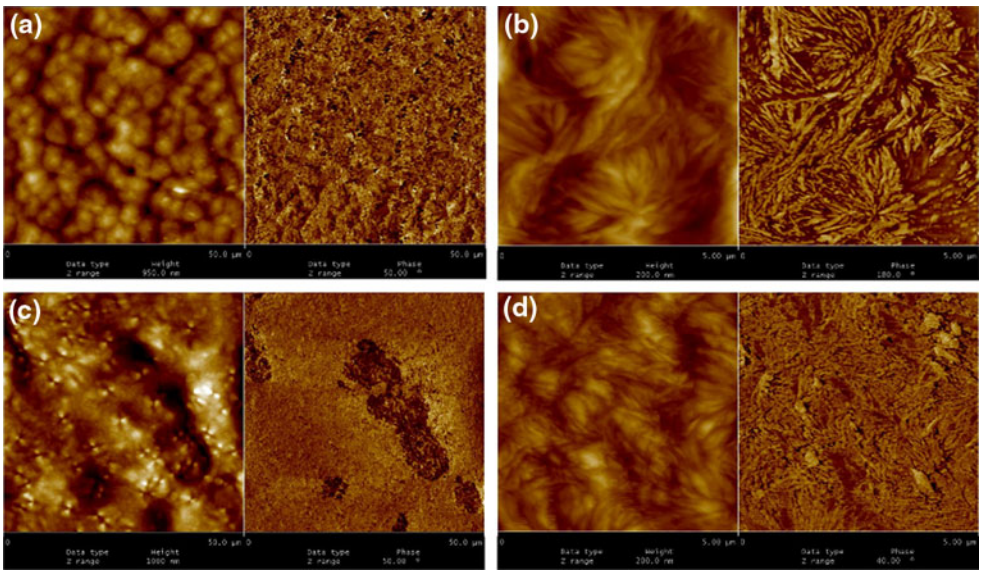

Fig. 4 AFM images of PLLA: **a**, **b** as cast, **c**, **d** sterilised in an autoclave at 120°C for 20 min. *Left* images are 50 μm scans and right ones are 5 μm scans

the result of the topography of the as cast and sterilized samples as revealed by the section analysis (see the selected areas in height images shown on the right hand side). It is concluded that the average height of the crystalline domains in as cast PLLA is about 200 nm while that in sterilized PLLA is about 400 nm.

3.2 In vitro cytotoxicity assessment by cytotoxicity assessment and direct contact assays

Regarding to the short-term extraction test, differences were observed on proliferation rates between the three types of cell lines cultured with respect to controls and

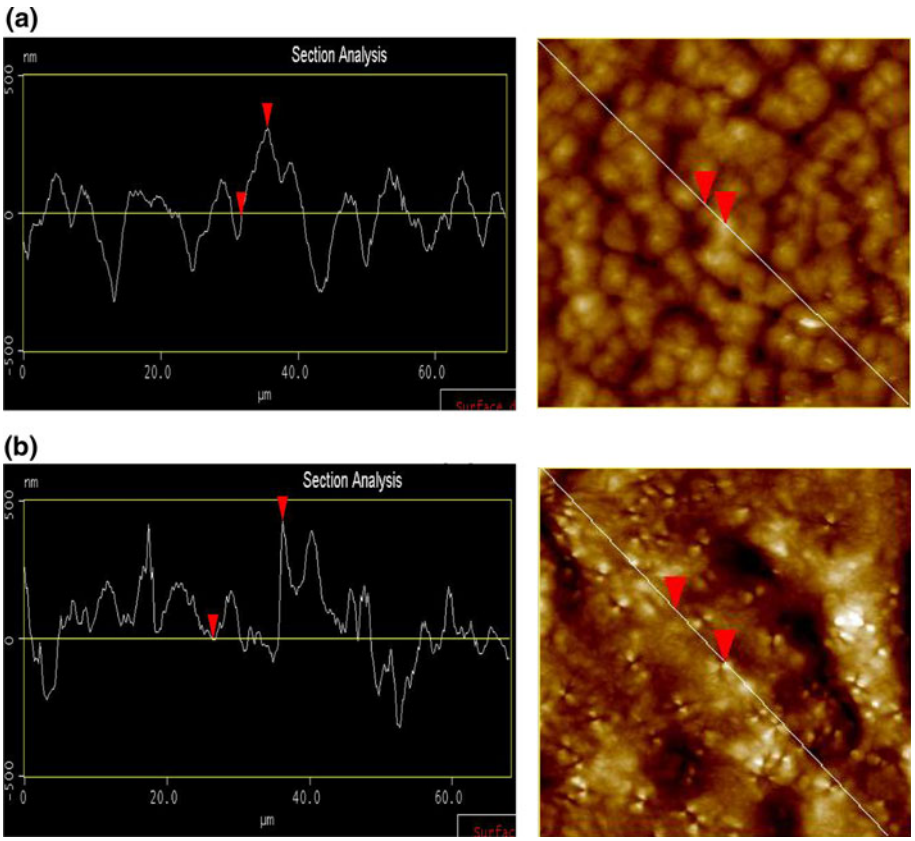

Fig. 5 AFM cross-section image (*left*) and height image (*right*) of PLLA: **a** as cast, **b** sterilised. Image size is 50 μm

cultures with sterilized materials extracts, as shown in Fig. 6a–c. It is remarkable the toxic effect of PVC as positive control in all cases since L929, neonatal fibroblasts and keratinocytes were not able to proliferate. The HDPE used as negative control and the polylactide materials induced different effects depending on cell type. The validity of the test can be confirmed by the considerably lower values obtained for the positive control, demonstrating that all cell types were susceptible to measurable degrees of cytotoxicity.

Figure 6a shows the optical density as determined by the colorimetric assay for different cell incubation times (for 24, 48, and 72 h) in the corresponding medium that has been put into contact with the different materials. As can be observed both the negative control and PLLA have already proliferated after 24 h incubation while PDLA and B5050 show similar values to those at time zero; however they have already proliferated after 48 h. Hence, PLLA, PDLA and PLLA/PDLA do not present any cytotoxic effect for L929 cells. On the contrary, a 1.2-fold increase in proliferation rate of PLLA-extracted medium compared with negative control was observed, approaching control values. When compared PDLA and B-5050-extracts with values for negative control at 72 h, no significant differences in proliferation rates were observed among them.

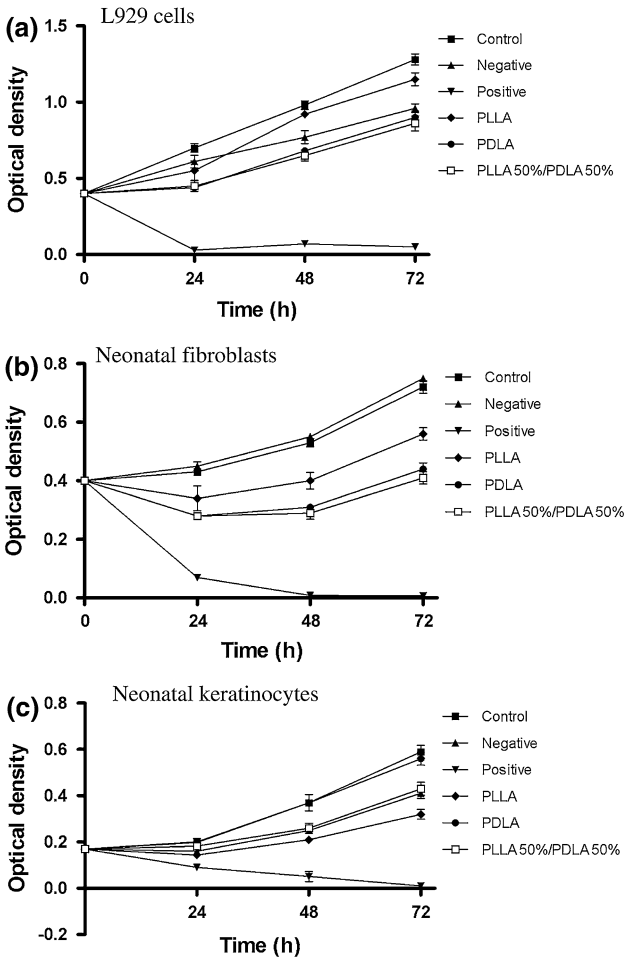

Fig. 6 Effect of PLLA, PDLA and B-5050 on proliferation rate: **a** L929 cells, **b** neonatal fibroblasts, **c** neonatal keratinocytes

Figure 6b shows the effect of PLLA, PDLA and B5050 on proliferation of neonatal fibroblast cells. It is noted that during the first period of 24 h the adaptation of cells to extractive media in all materials induces a transient inhibition of proliferation. However, from 24 to 48 h a 1.2-fold increase in cell population is observed in both control and PLLA-extracted-medium, whereas the cells treated with PDLA and B-5050 extracted medium do not proliferate (1.03-fold). From 48 to 72 h, the neonatal fibroblast population increases in all cases, 1.36-fold for the control and 1.4-fold for PLLA, PDLA and B-5050.

Figure 6c shows the effect of PLLA, PDLA and B5050 on proliferation of neonatal keratinocytes. In this case proliferation values in PDLA medium approaches those of control showing constant cell population between 0 and 24 h and the highest proliferation rate with respect to PLLA and B-5050 after 24 h. After 72 h a 1.3-fold increase of proliferation rate is observed for cells treated with PDLA-extracted medium. In the case of PLLA, and in spite of the fact that proliferation rate is slightly lower than that in control, significant differences were found when compared with positive control (32-fold increase at 72 h) demonstrating its viability. Concerning the cell proliferation values in B-5050 treated media no significant differences were found when compared with negative control.

Cell seeding assessment on polylactides was determined by scanning electron microscopy (SEM). SEM analysis was conducted to determine the cell morphology, spreading and adhesion of the different cells in contact with the different polylactides. Figure 7 shows the micrographs taken to L929 cells, neonatal fibroblasts and keratinocytes after 5 days of culture on PLLA, PDLA and B-5050. Particularly during the one-week culture period, L-929 started to colonize better on PLLA surface than on PDLA or B5050; moreover, images with high magnification show cells stretching and forming projections on the surface of assayed scaffolds at 72-h cultures. In the case of neonatal fibroblasts, the typical spindle shaped cell morphology was highly conserved. At the end of the first week, a cell monolayer was found in all of substrates for cell adhesion. Neonatal keratinocytes spread out homogenously on the surface of scaffolds showing epithelial features such as intercellular junctions and apparently good adhesion to substracts. Hence this results show a high degree of colonization on the surface of polylactides denoting that PLLA, PDLA and B-5050 are valid substrates for cell adhesion and proliferation.

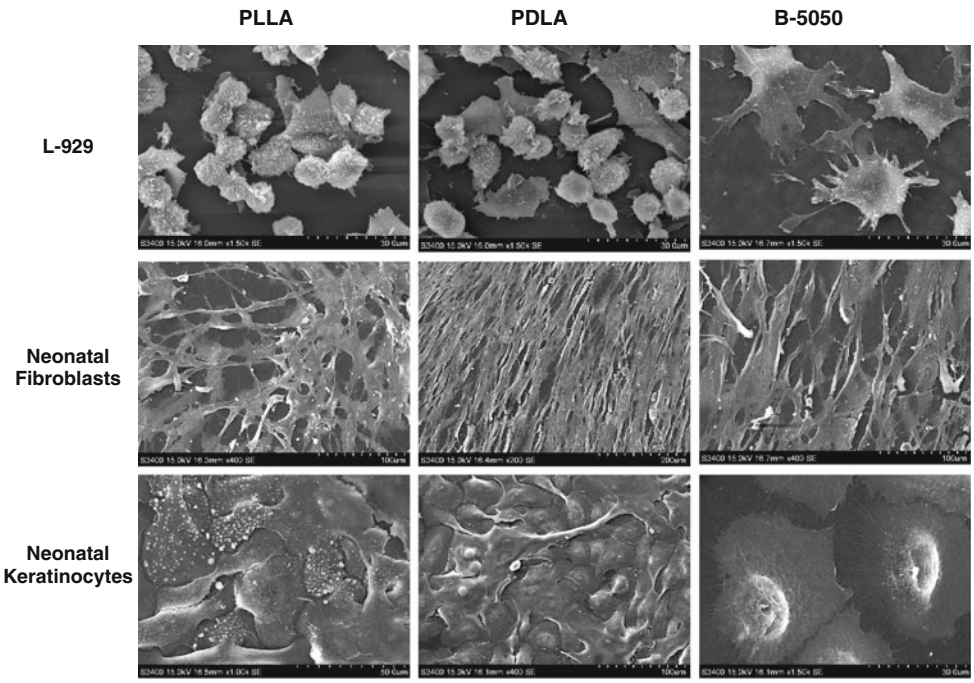

Fig. 7 Scanning electron microscopy (SEM) of L-929, human neonatal fibroblasts and keratinocytes cultured on PLLA, PLGA and B5050 scaffolds. As shown, the cells occupied homogenously most of the surface of biomaterials, the original phenotype of cells was highly conserved and where well adhered showing attached projections

4 Discussion

The uses of biodegradable polylactides as medical devices (implants, scaffolds or carriers for controlled antibiotic release) require not only the understanding of the relationships among composition and structure that result in different degradation profiles but also the understanding of cell–surface interactions in terms of adhesion, proliferation and differentiation. In consequence, the cellular response to drug delivery or scaffold systems that utilize biodegradable, biocompatible polymers such as polylactides are of paramount importance.

It is well known that the evolution of physical properties and biodegradability of polymer scaffolds depend on issues connected with crystallization. However little is known about crystallinity related aspects on cell behavior and biocompatibility. In this work the polylactide films obtained by solvent casting were sterilized in an autoclave before analyzing their interaction with cells. The DSC curves of PLLA and PDLA were presented in Fig. 1 before and after sterilization at 120°C during 20 min. Since this is a temperature higher than the glass transition of polylactide, sterilization led to an increase of crystallinity degree. Since PLLA and PDLA used in this work are both of high optical purity the crystallinity fraction obtained was very similar, about 30%, yet different melting temperatures resulted because of their different molecular weights.

When recrystallizing the as cast films under autoclave sterilization temperature conditions spherulitic morphology was revealed for PLLA. The AFM analysis revealed average thickness of lamellae of about 100–150 nm. Similar spherulitic morphology should be expected for the PDLA enantiomeric counterpart of PLLA, although thinner lamella would derive as a 10°C lower melting temperature was determined for the latter. The AFM investigations were conducted in this work with the aim of characterizing the crystalline polymer surfaces of films to be put into contact with cells for proliferation and adhesion analysis. The DSC analysis reveals the bulk crystallinity aspects of the films. However, in tissue engineering applications, though bulk properties remain important, surface properties play a greater role, since it will be the outer surface that will interact with cells, and crystalline aspects of the bulk and surface may present differences [32]. For example previous research suggests that PLLA microparticle of higher crystallinity elicited a smaller inflammatory response compared to lower crystallinity particles [33].

The effects of the crystallinity degree in optically pure polylactides (PLLA or PDLA) and stereocomplex crystallization on the physical properties of PLA have been extensively studied [41]. It is known that PLA stereocomplex crystals show slower thermal, hydrolysis, and enzymatic degradation rate, as well as better heat-resistance than the PLA homocrystals. This has been ascribed to the intermolecular specific interactions, tighter molecular packing, and smaller molecular mobility of the stereocomplex crystals. Upon the stereocomplex crystallization the tensile modulus also improves considerably compared to the PLLA or PDLA homocrystals. Hence stereocomplex crystallization has been considered as a promising approach to improve the physical properties of PLA materials.

In a recent work the chiral effects on the responses of osteoblastic cells to the polylactide substrates was reported [35]. The observation of cell morphologies revealed that PDLA films provided an unfavourable surface for cell attachment; in addition the racemic stereocomplex of PLLA and PDLA showed relatively higher positive effects on both cell growth and proliferation. Our study on the crystallinity effects of polymer substrates on cell behaviour further contributes to the understanding of polymer/cell interactions by extending the above mentioned studies to three other cell types: L929 fibroblasts and human neonatal fibroblasts and keratinocytes.

In our work both PLLA and PDLA crystallized as α homocrystals, and the equimolar PLLA/PDLA (B-5050) blend crystallized fully as stereocomplex following to a specific annealing treatment, were cell cultured after extraction from the extract fluid according to ISO 10993-12. The proliferation of cells after incubation in corresponding medium at 24, 48 and 72 h were presented in Fig. 6. The results obtained can thus be analyzed in the light of the effects of both the enantiomeric composition (chiral effects) and homocrystal versus sterocomplex crystallization of polylactides on fibroblasts L929 and human neonatal fibroblasts and keratinocytes proliferation.

Both L929 fibroblasts and neonatal fibroblasts present faster proliferation in PLLA than in PDLA extracts, in agreement with the results reported in the literature for osteoblasts [35]. However, far from being cytotoxic as it is the PVC positive control, PDLA shows a good cell response for both types of fibroblasts, although cell viability increases slower but approaching to that of PLLA after 3 days after extraction from the medium. In regard to the stereocomplexed equimolar polylactide, cell proliferation values stay somewhat in the order of that of PDLA, though with a trend to a slightly faster proliferation than with PDLA and showing no cytotoxicity.

It is also worth to be noted that both L929 and neonatal fibroblast proliferation was slower and final viability was smaller with all three polylactides studied than with the HDPE used as negative control in these tests. In contrast cytotoxicity assays with neonatal keratinocytes revealed a different behaviour. First the viability of all polylactides was larger than that of HDPE negative control. Second the viability and proliferation rate behavior of all three polylactide substrates studied was reversed from the behavior observed with fibroblasts since PDLA was the material showing the highest rate of proliferation and viability, PLLA the lowest, the enantiomeric stereocomplex blend staying in the middle.

It is remarkable that all cell types studied here showed a trend with the enantiomeric composition of the polylactide materials utilized in cytotoxicity tests with fibroblasts, showing larger viability and proliferation of fibroblasts with L-lactide chirality than with D-lactide chirality. In this sense a trend was also observed with keratinocites, yet the larger viability and proliferation was in this case observed for polylactides having larger amounts of D-lactide chirality. These results indicate that the biological response to chirality should be studied specifically for each type of cell without an a priori assumption that L-chirality should be better than D-chirality. Thus enantiomeric configurations of polylactide chains do not only play an important role in the resultant physical and mechanical properties but also in its biological responses when used in biomedical domains.

5 Conclusions

Crystallinity aspects derived from the complex stereochemistry of polylactides can be important factors affecting cell viability and adhesion when used in tissue engineering applications. By properly selecting the enantiomer composition and a blending/heat treatment strategy we have prepared polylactides having different crystalline characteristics. AFM revealed spherulites of 5–6 μm diameter with radial growth of edge on lamellae in as cast films with significant amount of non crystalline amorphous interlamellar and inter-spherulitic dark regions. However, the samples crystallised under sterilization conditions revealed larger crystallinity and a 3D sheaflike morphology constituted of axiallites. The equimolar blend was prepared by annealing at 190°C, a temperature higher than the melting temperature of the α crystal, leading to a stereospecific crystallization as stereocomplex. Although there is no cytotoxicity in any of the polylactide systems studied the different cells responded in a specific manner depending on the composition and the crystalline characteristics of the substrates. L-929 murine fibroblasts proliferated better in PLLA than in PDLA containing materials whereas keratinocyte proliferation was improved in PDLA. Hence compositional aspects determining the polylactide crystalline features should be specified to achieve the desired cell interactions for specific tissue engineering applications.

In vitro studies showed that, although we observed slight differences in proliferation rate between L929, neonatal fibroblasts and keratinocytes cultured on the three different materials, cells readily attach and grew on the scaffolds. However, due to different response of each type of cell to different materials, additional investigations should be made in order to determine the characteristics of each material for the precise clinical use.

Acknowledgments The authors are thankful for financial support from the Basque Government Department of Education, University and Research (consolidated research groups GIC10/152-IT-334-10 and project IT431-07) and Department of Health (PI2005111043). We also thank SGIKER from UPV/EHU for WAXD and SEM

measurements and the support of *CIC Biomagune* and *Biobasque* agency (Project Etortek IE07-201).

References

1. Langer R, Vacanti JP. Tissue engineering. Science. 1993;260: 920–6.
2. Yang S, Leong K, Du Z, Chua C. The design of scaffolds for use in tissue engineering. Part I. Traditional factors. Tissue Eng. 2001;7:679–89.
3. Takezawa T. A strategy for the development of tissue engineering scaffolds that regulate cell behavior. Biomaterials. 2003;24: 2267–75.
4. Salgado AJ, Coutinho OP, Reis RL. Novel starch-based scaffolds for bone tissue engineering: cytotoxicity, cell culture, and protein expression. Tissue Eng. 2004;10:465–74.
5. Thomsom RC, Mikos AG, Beahm E, Lemon JC, Saterfield WC, Aufdemorte TB, Miller MJ. Guided tissue fabrication from periosteum using preformed biodegradable polymer scaffolds. Biomaterials. 1999;20:2007–18.
6. Navarro M, Ginebra MP, Planell JA, Zeppetelli S, Ambrosio L. Development and cell response of a new biodegradable composite scaffold for guided bone regeneration. J Mater Sci Mater Med. 2004;15:419–22.
7. Ren J, Ren T, Zhao P, Huang Y, Pan K. Repair of mandibular defects using MSCs-seeded biodegradable polyester porous scaffolds. J Biomater Sci Polym Ed. 2007;18:505–17.
8. Wang S, Cui W, Bei J. Bulk and surface modifications of polylactide. Anal Bioanal Chem. 2005;381:547–56.
9. Reis RL, Cunha AM. Starch and starch based thermoplastics. Biological and biomimetic materials. Amsterdam: Pergamon-Elsevier Science; 2001. p. 8810–6.
10. Vainionpaa S, Rokkanen P, Tormala P. Surgical applications of biodegradable polymers in human tissues. Prog Polym Sci. 1989; 14:679–716.
11. De Jong WH, Eelco Bergsma J, Robinson JE, Bos RM. Tissue response to partially in vitro predegraded poly-L-lactide implants. Biomaterials. 2005;26:1781–91.
12. Okamoto Y. "Trends in polymer science" chiral polymers. Prog Polym Sci. 2000;25:159–62.
13. Sarasua JR, Prud'homme RE, Wisniewski M, LeBorgne A, Spassky N. Crystallization and melting behaviour of polylactides. Macromolecules. 1998;31:3895–905.
14. Södergard A, Stolt M. Properties of lactic acid based copolymers, their correlation with composition. Prog Polym Sci. 2002;27: 1123–63.
15. De Santis P, Kovacs AJ. Molecular conformation of poly(S-lactid acid). Biopolymers. 1968;6:299–306.
16. Okihara T, Tsuji M, Kawaguchi A, Katayama K, Tsuji H, Hion H, Ikada Y. Crystal structure of stereocomplex of poly(L-lactide) and poly(D-lactide). J Macromol Sci B. 1991;30:119–40.
17. Ikada Y, Jamshidi K, Tsuji H, Hyon SH. Stereocomplex formation between enantiomeric poly(lactides). Macromolecules. 1987; 20:904–6.
18. Brizzolara D, Cantow HJ, Diedericks K, Seller E, Domb J. Mechanism of the stereocomplex formation between enantiomeric poly(lactides)s. Macromolecules. 1996;29:191–7.
19. Sarasua JR, López-Rodríguez N, López-Arraiza A, Meaurio E. Stereoselective crystallization and specific interactions in polylactides. Macromolecules. 2005;38:8362–71.
20. Sarasua JR, López-Arraiza A, Balerdi P, Maiza I. Crystallization, thermal behaviour of optically pure polylactides, their blends. J Mater Sci. 2005;40:1855–62.
21. Sarasua JR, López-Arraiza A, Balerdi P, Maiza I. Crystallization, mechanical properties of optically pure polylactides, their blends. Polym Eng Sci. 2005;45:745–53.
22. Li S, McCarthy S. Further investigations on the hydrolytic degradation of poly(DL-lactide). Biomaterials. 1999;201:35–44.
23. Tsuji H, Miyauchi S. Poly(L-lactide): VI effects of crystallinity on enzymatic hydrolysis of poly(L-lactide) without free amorphous region. Polym Degrad Stabil. 2001;71:415–24.
24. Tsuji H. In vitro hydrolysis of blends from enantiomeric poly(lactide)s. Biomaterials. 2003;24:537–47.
25. Karst D, Yang Y. Molecular modelling study of the resistance of PLA to hydrolysis based on the blending of PLLA and PDLA. Polymer. 2006;47:4845–50.
26. Bernal-Lara TE, Liu RF, Hiltner A, Baer E. Structure and thermal stability of polyethylene nanolayers. Polymer. 2005;46:3043–55.
27. Kikkawa Y, Abe H, Fujita M, Iwata T, Inoue Y, Dói Y. Crystal growth in poly(L-lactide) thin film revealed by in situ atomic force microscopy. Macromol Chem Phys. 2003;204:1822–31.
28. Meaurio E, López-Rodríguez N, Sarasua JR. Infrared spectrum of poly(L-lactide): application to crystallinity studies. Macromolecules. 2006;39:9291–301.
29. Fischer EW, Stertzel HJ, Wegner G. Investigation of the structure of solution grown crystals of lactide copolymers by means of chemicals reactions. Kolloid Z Z Polym. 1973;251:980–90.
30. Nakagawa M, Teraoka F, Fujimoto S, Hamada Y, Kibayashi H, Takahashi J. Improvement of cell adhesion on poly(L-lactide) by atmospheric plasma treatment. J Biomed Mater Res B. 2006;77: 112–8.
31. Yamaguchi M, Shinbo T, Kanamori T, Wang PC, Niwa M, Kawakami H, Nagaoka S, Hirakawa K, Kamiya M. Surface modification of poly(L-lactic acid) affects initial cell attachment cell morphology, and cell growth. J Artif Organs. 2004;7:187–93.
32. Park A, Cima LG. In vitro cell response to differences in poly (L-lactide) crystallinity. J Biomed Mater Res B. 1996;31:117–30.
33. Biggs DL, Lengsfeld CS, Hybertson BM, Ka-yun NG, Manning MC, Randolph TW. In vitro, in vivo evaluation of the effects of PLA microparticle crystallinity on cellular response. J Control Release. 2003;92:147–61.
34. Lee J, Cuddihy MJ, Kotov NA. Three-dimensional cell culture matrices: state of the art. Tissue Eng Part B. 2008;14:61–86.
35. Yi Q, Xintao W, Li L, He B, Nie Y, Wu Y, Zhang Z, Gu Z. The chiral effects on the responses of osteoblastic cells to the polymeric substrates. Eur Polym J. 2009;45:1970–8.
36. ISO document 10993-12 Biological compatibility of medical devices. Sample Preparation and Reference Materials 1992.
37. ISO document 10993-5 Biological compatibility of medical devices. Test for cytotoxicity: in vitro methods. 1992.
38. Chen H, Cebe P. Investigation of the rigid amorphous fraction in Nylon-6. J Therm Anal Calorim. 2007;89:417–25.
39. Ohtani Y, Okumura K, Kawaguchi A. Crystallization behavior of amorphous poly(L-lactide). J Macromol Sci B. 2003;42:875–88.
40. Sperling LH. Introduction to physical polymer science. New York: Wiley; 1992.
41. Pan P, Inoue Y. Polymorphism and isomorphism in biodegradable polyesters. Prog Polym Sci. 2009;34:605–40.